

Performance Evaluation of Band-Notch Techniques for Printed Dual Band Monopole Antennas

Khalil H. Sayidmarie*, Tariq A. Najm

Department of Communication Engineering, College of Electronic Engineering, University of Mosul, Mosul, Iraq

Abstract Three methods for band-notching in printed monopole antennas are investigated. A dual band monopole antenna in the form of double rectangular rings is considered in the investigation. The antenna covers the frequency bands of the IEEE 802.11a/b/g standard (2.4-2.48GHz, 5.15-5.35GHz and 5.725-5.825GHz), while a notch in the frequency range of 4-5 GHz is implemented. The performances of each of the three band notching techniques against various parameters are shown. The overall performance of the band-notch techniques using; parasitic element, slots, and stubs are compared. The CST microwave software package has been used in the investigations.

Keywords Band-notched Antennas, Dual Band Antennas, Planar Monopole Antennas, WLAN Antennas

1. Introduction

The rapid growth of modern wireless communication systems such as smart phones, GSM, UMTS, LTE, and WLAN has motivated the research into suitable antennas suitable for these systems. Many of the modern wireless devices can incorporate more than one system, operating at different frequencies or spanning a very wide bandwidth. However, over the desired operational bandwidth, there may be some narrow bands occupied by other co-existing wireless systems. These co-existing systems can cause interference, and hence their frequencies should be blocked by either a band-reject filter or by some other techniques. On the other hand, to minimize noise effects, a multiband antenna system is preferred to receive minimal signal at frequencies in-between bands. Another requirement for a band notching is to prevent sensitive components, within the front-end of the receiver, from being overloaded by strong signals. Instead of deploying more than one antenna in such wireless devices, multiband antennas have found extensive use in these devices. These antennas should offer filtering properties not only to remove the effect of interference but also to get rid of additional bandstop filters, that are required to reject signals at unwanted frequencies. Therefore, various antennas with single or multiple notch functions have been developed for UWB communication systems, and WLAN systems[1]-[8].

One of the main conventional techniques for achieving band-notch characteristics is the use of slots or slits of various shapes. The slots can be deployed in; the radiating

patch[6, 9], the feed line[7, 8], or the ground plane[10, 11]. The slots or slits are made to resonate at the notch frequency, resulting in disturbance of the current distribution on the radiating element, or reduce matching with the feed line. An alternative approach is to introduce parasitic elements adjacent to the radiating patch[12-14] or the feed line[15, 16]. The parasitic elements are made to resonate at the notch frequency where maximum energy is coupled to them. Consequently, there will be disturbance in the current distribution across the radiating element. The parasitic element, when placed adjacent to the feed line, receives coupled energy when it resonates at the notch frequency, and thus changes the input impedance of the antenna. The third approach is to attach a stub either to the feed-line or to the radiating patch[17-18]. The stub is well known for its use in matching, however, it should be noted that in this paper, it is rather used to produce adequate mismatch at the notch-frequency.

A segmented structure was recently proposed as a versatile approach to reject certain band of UWB printed monopole antennas. The method was implemented on circular, beveled rectangular, and regular hexagonal shaped monopole antennas[19]. By segmenting the radiating patch into three parts, intensive coupling occurs between the fed segment at the center of antenna and the two parasitic side segments at the target frequency, and consequently the band-notched property is obtained. It is worthy to mention that such segmentation or chopped process has been recently proposed to enhance the phase response of reflectarray elements[20]. A compact planar monopole UWB antenna of a spade-shaped radiation patch with four tunable notched bands has been proposed in[21]. The antenna employs three crescent-shaped parasitic resonators on the back side and an inverted U-slot in the ground plane, thus employing two of the band-notch techniques simultaneously. Another example

* Corresponding author:

kh.sayidmarie@gmail.com (Khalil H. Sayidmarie)

Published online at <http://journal.sapub.org/ijea>

Copyright © 2013 Scientific & Academic Publishing. All Rights Reserved

of using a slot in the radiating patch, and two parasitic open-rings adjacent to the ground plane has been presented in[22]. The parasitic elements have also been arranged in multilayer configuration as in[23] where four notched-bands have been achieved.

In this paper, a compact monopole antenna consisting of dual rectangular rings, and a 50-Ohm microstrip feed line is investigated for the implementation of various band-notch techniques. It should be emphasized that the results reported in this paper are generated using the CST software package which is used in the design and parametric studies of the investigated antennas. Three band-reject techniques are studied thoroughly, where the effect of various parameters on the performance are investigated. The study aims at comparing the performance and capability of the investigated techniques. The paper is arranged as the following. After an introductory section, the design of dual ring antenna, considered in the investigations, is presented. Sections 3 to 5 present results of investigating the three notch techniques. Section 6 gives comparison of the obtained results, while section 7 lists the conclusions.

2. Antenna Design

The antenna considered in the investigation of the band notch techniques is a dual band monopole antenna presented recently in[24]. This antenna, which uses two concentric rectangular rings, deploys the self similarity property of the fractal geometry to implement dual-band operation. The dimensions of the two rings were initially chosen such that the mean circumference of each ring corresponds to the effective wavelength at the center of each of the wanted frequency bands. Thus the outer ring corresponds to the lower band while the inner ring corresponds to the upper band. The antenna is simulated using FR-4 substrate with a dielectric constant of 4.4, thickness of 1.6 mm, and a loss tangent of 0.025. The width of the feed line for each antenna was fixed at 3.2 mm to implement 50 Ohm characteristic impedance of the SMA connector, and the length of the feed was put at $L_f=17\text{mm}$ to function as a $\lambda/4$ transformer at the lower band frequency. The effective wavelength in the dielectric substrate ϵ_e was calculated as[25]:

$$\epsilon_e = \frac{\epsilon_r + 1}{2} \quad (1)$$

Table 1. Detailed parameters of the dual rectangular ring antenna. All dimensions are in millimeters

L_1	L_2	L_3	L_4	W_1	W_2	L_f	W_f	L_g	U
26	17	15.6	10.2	2.25	1.4	18	3.2	17	5

The antenna is shown in Fig. 1, and its parameters are shown in Table (1). It was shown that tapering the ground plane by cutting two triangles from the upper corners of the ground plane produces better response[24]. The tapering results in an increase in the separation between ground plane and lower side of the outer ring thus allowing better current

distribution along this edge. The antenna was simulated using the CST software, and the investigated band-notch techniques are presented in the following sections.

3. Using Parasitic Elements

In this method of band rejection, a certain piece of conducting strip is placed adjacent to the radiating element [12],[16],[26-27]. This added element is called "Parasitic" since it is not directly fed as for the radiating element. The element is designed to resonate at the desired notch frequency.

Due to its proximity to the radiating element, the energy is maximum at the resonance frequency. Hence, the current distribution across the radiating element is disturbed leading to reduced gain or increased reflection at the resonance frequency. The notch behavior is exhibited as increased reflection coefficient at the notch frequency. Applying this idea to the dual band dual ring antenna, presented in[24], a modified design is proposed here. The geometry of the dual rectangular ring antenna with the two proposed L-shaped parasitic elements is shown in Fig.(2). The dual rectangular ring radiation patch and the microstrip feed line are etched on the same surface of the substrate, while the tapered rectangular ground and the two L-shaped parasitic elements lie on the opposite surface of the substrate. The parameters of this design are provided in Table (1), and Fig.2-c. The investigations started with studying the effect of varying the length L_p of the two parasitic L-shaped arms, whereas the separation d was set equal to zero ($d=0$). The reflection coefficient response for various values of the length L_p , when $d=0$, are shown in Fig. (3). It can be seen that without the parasitic elements ($L_p=0$), there is no notch in the response at the frequency range of 4-5 GHz. At the notch frequency, the L-shaped line can be considered as a transmission line open-circuited at both of its ends. When the length L_p is increased, the center frequency of notch decreases. The obtained results along with length of parasitic element L_p and S_{11} achieved are shown in Table (2). It can be seen that at the notch frequency F_n , the length of the parasitic element is almost equal to the effective wavelength, as obtained using Eq. (1). This indicates that, at the notch frequency this element is resonating and leading to a mismatch of the antenna. The reflection coefficients (for various lengths) at F_n were higher than -4.9dB indicating that at least 25% of the incident power is reflected back. In other words, the reflection coefficient has increased by about 13.5dB in comparison with the case without notching.

To obtain better insight into the band-notch operation of the parasitic element, the surface current distribution across the antenna rings and the parasitic element was found using the CST software at $F_n=4.5\text{GHz}$ (when $L_p=39$), is shown in Fig.(4). It can be seen that the current distribution along the parasitic element at the notch frequency is richer than those at other elements, proving that it is at resonance.

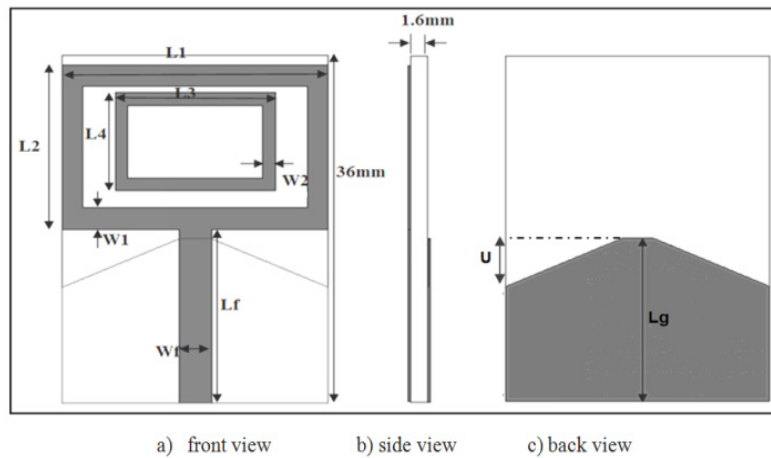


Figure 1. Geometry of the dual rectangular ring antenna[24]

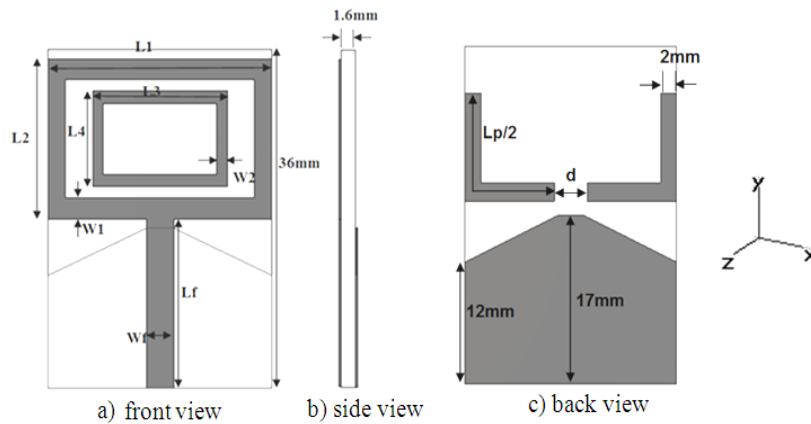


Figure 2. Geometry of dual rectangular ring antenna with parasitic element

For further evaluation, the three dimensional variation of radiated field at the notch frequency is shown in Fig.(5).

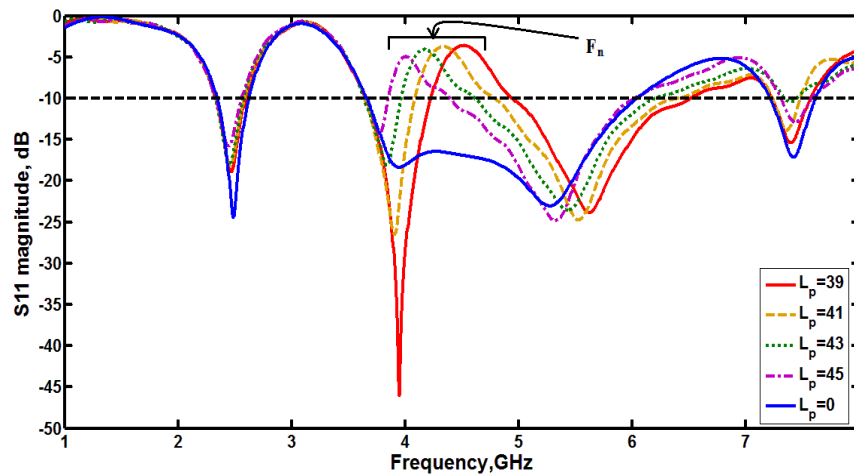


Figure 3. Reflection coefficient of the dual rectangular antenna with parasitic element showing effect of varying the value of L_p whereas the distance $d=0$

Table 2. Frequency characteristics calculated from the results of Fig. (3)

L_p (mm)	F_n (GHz)	λ_{dn} (mm)	L_p/λ_{dn}	S_{11n} (dB)
0	---	---	---	---
39	4.5	40.57	0.961	-3.6
41	4.33	42.16	0.972	-3.7
43	4.15	44	0.977	-4
45	4	45.7	0.984	-4.9

The realized gain at boresight descends to the value of (-2.03dB_i) because the efficiency at the notch frequency (4.5GHz) decreased to (16.4%).

Next a study was made by fixing the length at $L_p/2=19.5\text{mm}$, while considering various values of (d) (the gap between the two L-shaped arms). The reflection coefficient characteristics for various values of (d) are shown

in Fig.(6). The reflection coefficient at the notch frequency decreased slightly as the separation d was increased. The result can be attributed to the fact that with the gap, each arm resonates at the effective half wavelength. Since $L_p/2$ was kept constant, the notch frequency slightly changes due to some coupling at the ends of the two arms.

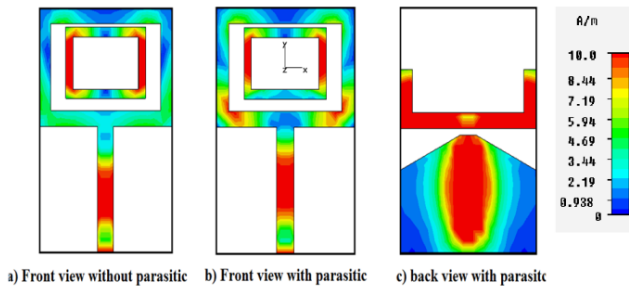


Figure 4. Surface current distributions of the dual rectangular ring antenna with parasitic element as obtained from the CST software, at the notch frequency ($F_n=4.5\text{GHz}$)

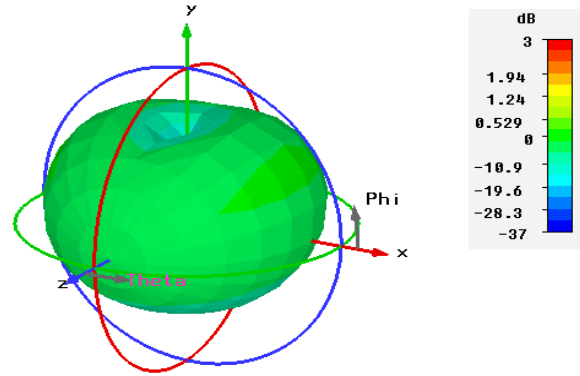


Figure 5. The three dimensional far-field radiation pattern at notch frequency of $F_n=4.5\text{GHz}$

Table 3. Frequency characteristics taken from the results of Fig.(6)

$d(\text{mm})$	$F_n(\text{GHz})$	$\lambda_{dn}(\text{mm})$	(L_p+d/λ_{dn})	$S_{11n}(\text{dB})$
0	4.5	40.6	0.96	-3.6
2	4.36	41.9	0.97	-3.6
4	4.36	41.9	1.02	-4.2
6	4.31	42.4	1.06	-4.6

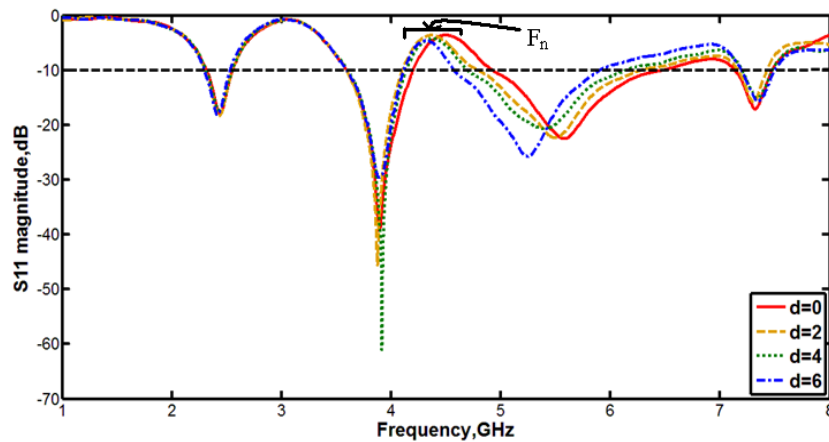


Figure 6. Reflection coefficient of the dual rectangular antenna with parasitic element showing effects of varying the distance d whereas $L_p/2=19.5\text{mm}$

4. U-Shaped Slot

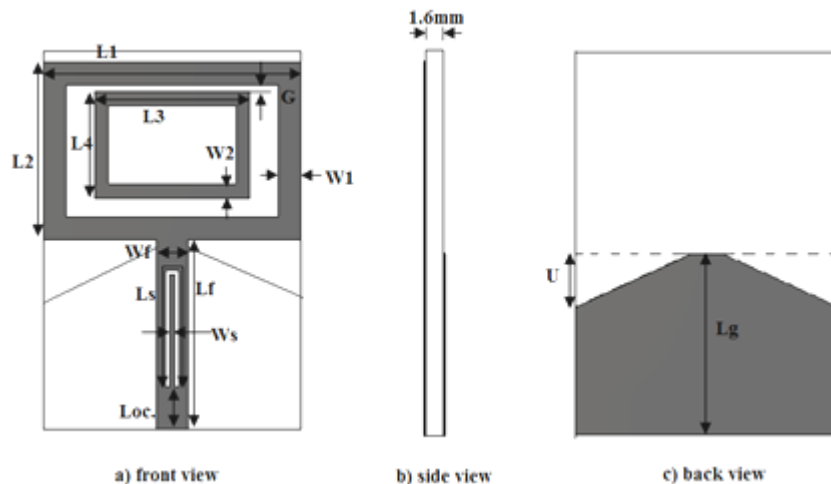


Figure 7. Geometry of rectangular antenna with the use of U-slot

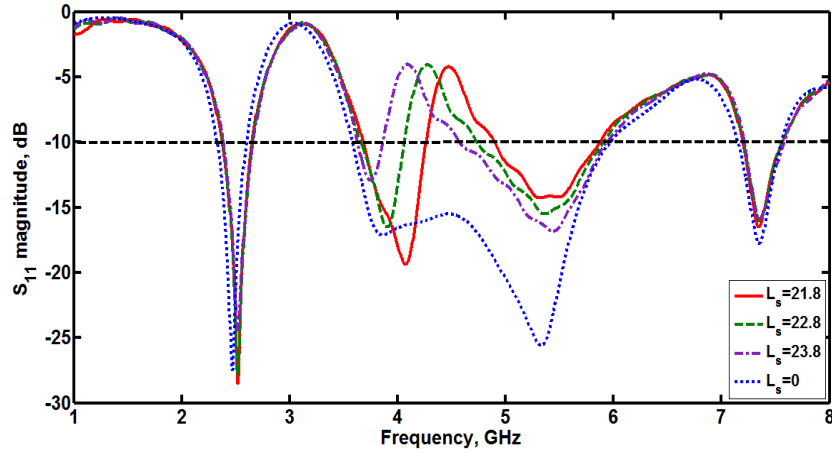


Figure 8. Reflection coefficient of the rectangular antenna with the U-slot showing effects of varying slot length L_s whereas $W_s=0.8$ and slot width $h=0.4$ mm

In this method of band rejection, a strip in the form of U-shape is removed from the feed line[6-11],[28]. The formed U-shaped slot represents a half-wavelength resonator with two short circuited ends. Due to the half-wavelength transformer action the surface current will be reflected, and this decreases the radiation. The U-slot is designed to resonate at the desired notch frequency, and this method is utilized here to implement a notch band for the dual rectangular ring antenna considered in section 2. The geometry of the rectangular ring antenna with the use of U-shaped slot in the feeder is shown in Fig.(7). The parameters of this design are shown in Table (1) and Fig. (7).

To adjust the notch band frequency to a certain value without varying the width of the band, different values of slot length L_s were considered while the slot width W_s was kept constant at 0.8mm. The obtained reflection coefficient characteristics are shown in Fig.(8). It is obvious that without slot ($L_s=0$), there is no notch behaviour in the response. The notch frequency decreases with increasing L_s . Table (4) compares parameters of the responses of Fig.(8). It shows that the slot length L_s , at the notch frequency, is approximately equal to half the effective wavelength in the dielectric substrate. The reflection coefficient values at F_n are now higher than -4.2dB while they were lower than -15dB before implementing the slot. Therefore, at the notch frequency, at least 25% of the incident power is reflected back.

The surface current distributions across the antenna with and without slot were studied using the CST software. The obtained current distributions at the notch frequency, $F_n=4.48$ GHz or when $L_s=21.8$, are shown in Fig.(9). It can be seen that the fed current along the U-shaped slot is reflected to the source leaving lower current at the radiating rectangular monopole. For further evaluation, the three dimensional far-field radiation pattern at the notch frequency is plotted in Fig.(10). The boresight realized gain at the notch frequency (4.48GHz) descends to the value of (-1.08dB_i)

since the efficiency decreased to (19.4%).

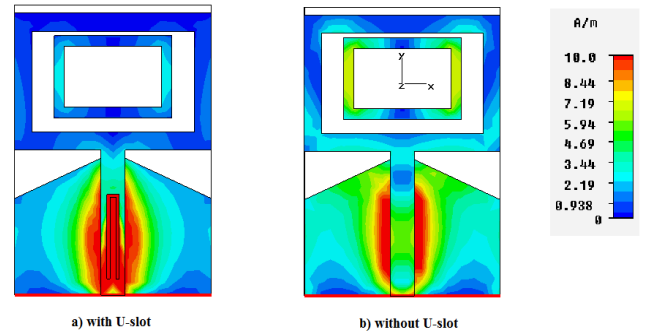


Figure 9. Surface current distributions of the rectangular antenna with U-slot in the feed line

Table 4. Frequency characteristics taken from the results of Fig(9)

L_s (mm)	F_1 (GHz)	F_L-F_U	F_n (GHz)	S_{11n} (dB)	$L_s/(\lambda_{dn}/2)$
0	2.48	2.34-2.61	---	---	---
21.8	2.51	2.38-2.65	4.48	-4.2	1.16
22.8	2.51	2.38-2.65	4.26	-4	1.16
23.8	2.51	2.38-2.65	4.08	-4	1.16

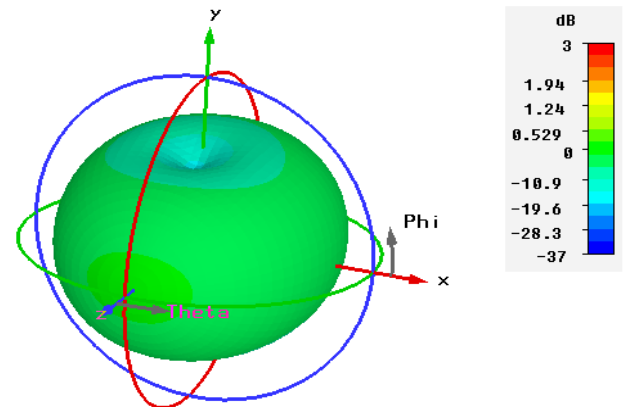


Figure 10. The three dimensional far-field radiation pattern at $F_n=4.7$ GHz

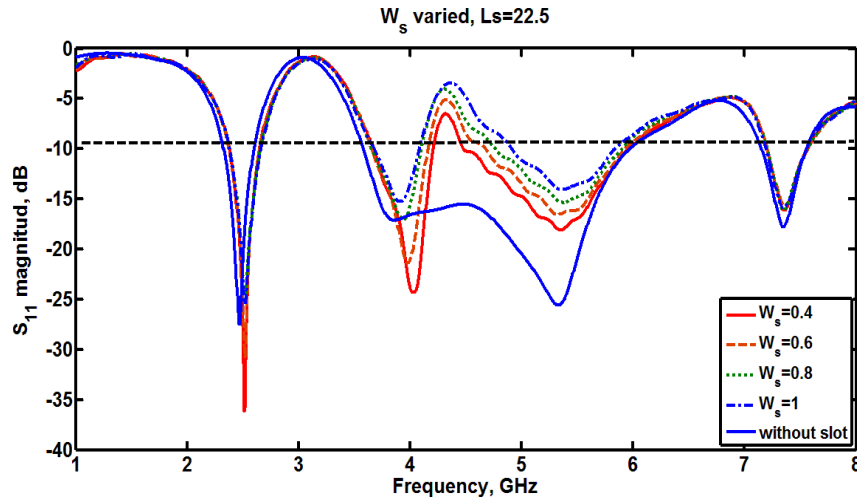


Figure 11. Reflection coefficient of the rectangular antenna with the U-slot showing the effects of varying slot width W_s whereas $L_s=22.5$ mm

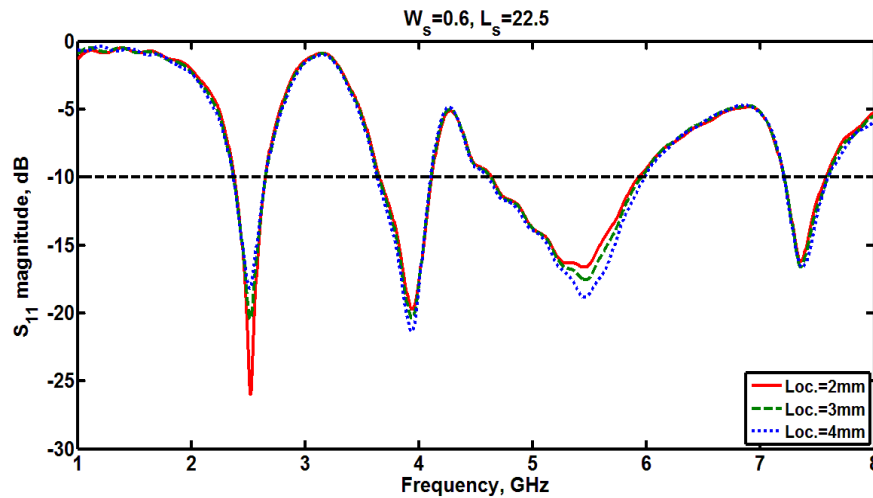


Figure 12. Reflection coefficient for several locations of the U-slot along the feed line. $L_s=22.5$, $W_s=0.6$

Table 5. Frequency characteristics taken from the results of Fig. (11)

W_s (mm)	F_1 (GHz)	$F_{1L}-F_{1U}$ (GHz)	F_n (GHz)	$F_{nL}-F_{nU}$ (GHz)	S_{11n} (dB)
0.4	2.5	2.37-2.64	4.32	4.2-4.48	-6.5
0.6	2.51	2.37-2.64	4.32	4.157-4.68	-5.09
0.8	2.51	2.37-2.64	4.31	4.1-4.76	-4.06
1	2.51	2.37-2.64	4.36	4.08-4.92	-3.43

To explore the effect of the slot width W_s , several values of W_s were considered while the length was kept constant $L_s=22.5$ mm and the obtained results are shown in Fig.(11). It is clear that increasing the value of W_s leads to improved notch performance, where the reflection coefficient goes up at the notch frequency, while the bandwidth of second band decreased. The value of notch frequency is not affected by varying the slot width. Therefore, the band notch characteristic may not only be affected by the length, and the width of the slot but also by the location L_{loc} of the slot along the line. Different values of L_{loc} were considered in the investigation to illustrate this effect as shown in Fig. (12). It is clear that changing the location of the slot has little effect on the reflection coefficient response and almost no effect on

the first and second bands.

5. The $\lambda/4$ Stub

A stub with an open end etched on the side of the feed line with a length approximately equal to quarter of the effective wavelength is the third method used for band rejection [17,18]. At resonance the open-circuit stub forms a short circuit at the feed line, thus reducing the power supplied to the antenna. The input impedance of an open circuited transmission line of length L is given by[29].

$$Z_{in} = -jZ_o \cot(B_g L) = -jZ_o \cot\left(\frac{2\pi L}{\lambda_g}\right) \quad (2)$$

At notch frequency, the stub is designed to resonate by setting its length to $(L=\lambda_g/4)$, then the value of Z_{in} approaches zero ideally and it is very small practically, thus short-circuiting the feed line.

The geometry of dual rectangular ring antenna with $\lambda/4$ stub connected to its feed line is shown in Fig.(13). The dual rectangular ring radiation patch, the microstrip feed line, and the $\lambda/4$ stub are etched on the same surface of the substrate,

and the tapered rectangular ground plane are on the opposite surface of the substrate. The parameters designed antenna are shown in Table (1), and Fig. (13).

The reflection coefficient responses for four different lengths L_{stub} of the stub are shown in Fig.(14), where it is clear that when the length of the stub is increased the notch frequency decreases. The frequency characteristics obtained from the results of Fig.(14) are summarized in Table (6). The table illustrates that the wavelength in the dielectric substrate divided by four i.e ($\lambda_d/4$) is approximately equal to the length of the stub at notch frequency. The use of $\lambda/4$ stub yield a reflection coefficient value of -1.9dB at the notch frequency $F_n=4.81\text{GHz}$ indicating that 65% of the incident power is reflected back. It can be seen that by varying the length of the stub, the reflection coefficient response is changed only around the notch frequency with very little effect on the two desired bands.

The surface current distribution across the antenna, with the $\lambda/4$ stub, was obtained using the CST software. The current distributions at notch frequency $F_n=4.39\text{GHz}$ (when $L_{\text{stub}}=10\text{mm}$) are shown in Fig.(15). It can be seen that the current distribution along the $\lambda/4$ stub is the richest at the notch frequency while the two rings have very little current as compared to the case with no stub. For further evaluation,

the three dimensional far-field radiation pattern at the notch frequency is shown in Fig.(16). The gain decreases to a value of (-1.9dB) while the efficiency at the notch frequency was reduced to (8.8%). The use of the stub has increased S_{11} at 4.5GHz from -15 dB to -1.9dB.

Table 6. The frequency characteristic of varying the length of the stub

L_{stub} (mm)	F_1 (GHz)	F_n (GHz)	S_{11n} (dB)	λ_{dn} (mm)	$L_{\text{stub}}/(\lambda_{dn}/4)$
0	2.47	---	---	---	---
9	2.4	4.81	-1.9	34.84	1.033
9.5	2.4	4.58	-1.9	36.6	1.038
10	2.4	4.39	-1.8	38.2	1.047
10.5	2.4	4.21	-1.8	39.68	1.058

The width of the stub is another parameter by which the width of the notch band can be adjusted. In Fig.(17) the length of the $\lambda/4$ stub was fixed at 10mm, while different widths were considered and the reflection coefficient illustrates that when the stub width gets wider the notch bandwidth increases. Detailed parameters of the obtained results of Fig.(17) are depicted in Table (7). It is obvious that the width of notch band increases with stub width and also the reflection coefficient improves.

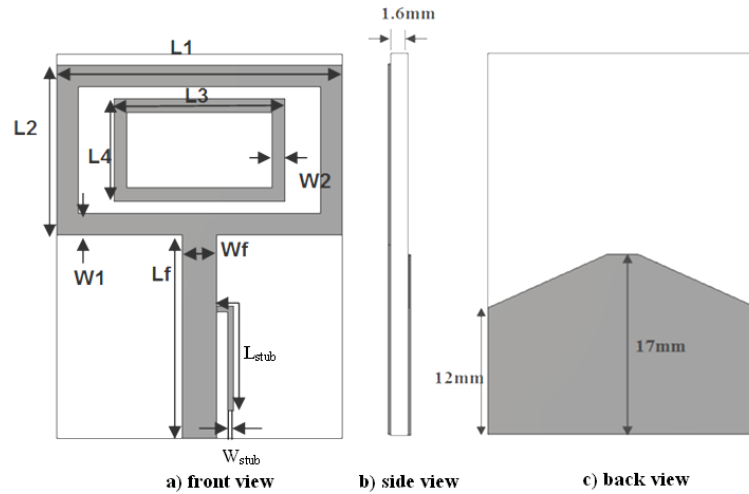


Figure 13. Geometry of dual rectangular ring antenna with $\lambda/4$ stub for band-reject purpose

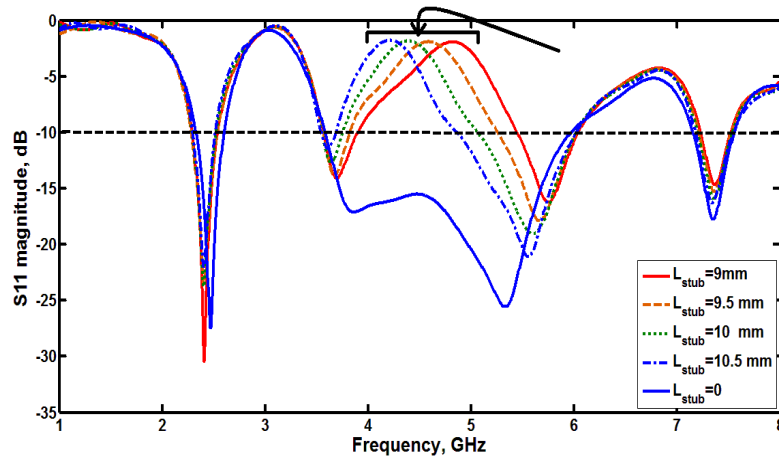


Figure 14. Reflection coefficient characteristics for four different stub lengths

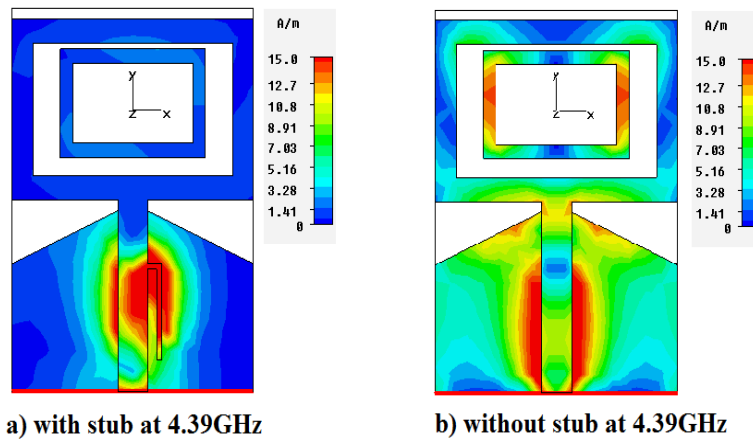


Figure 15. Surface current distributions of the investigated rectangular dual ring antenna; (a) with $\lambda/4$ stub, (b) without stub

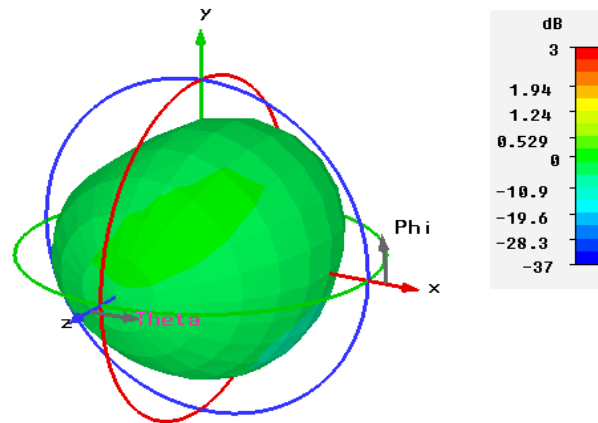


Figure 16. The three dimensional far-field radiation pattern at $F_n=4.39\text{GHz}$ with the $\lambda/4$ stub in the right side of the feed line as obtained from the CST

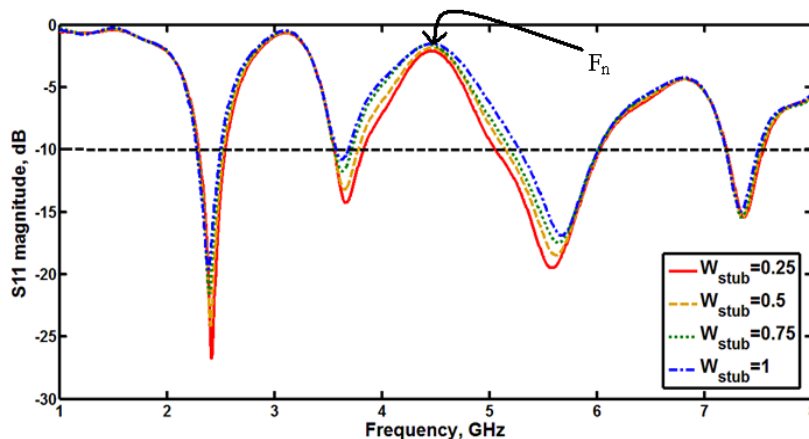


Figure 17. Reflection coefficient characteristic for different widths of the $\lambda/4$ stub. $L_s=10\text{mm}$, $F_n=4.46$

Table 7. Frequency characteristics obtained by varying the width of the $\lambda/4$ stub

W_{stub} (mm)	F_1 (GHz)	F_n (GHz)	S_{11n} (dB)	$F_{L1n}-F_{U1n}$ (GHz)	BW (GHz)
0.25	2.41	4.46	-2.1	3.82-5.06	1.24
0.5	2.4	4.46	-1.85	3.77-5.15	1.38
0.75	2.39	4.46	-1.61	3.71-5.19	1.48
1	2.37	4.46	-1.54	3.68-5.27	1.59

5.1. The Effect of Stub Shape and its Position along the Feed Line

To demonstrate the effect of stub position, three different locations of the stub along the feed line were considered. The obtained reflection coefficient results are shown in Fig. (19). When the stub is placed near the feed point the second band almost vanished, while moving the stub away from the feed point the response improved, illustrating that the stub and

feed line operate as transmission line matching elements as expected.

The geometry of the $\lambda/4$ stub was also studied and the obtained results for the three shapes, shown in Fig.(20), are

depicted in Fig.(21). Figure (21) demonstrates that the L-shape yields the best results. The little effect on the first band and the narrower band-notch made the L-shape as the better choice.

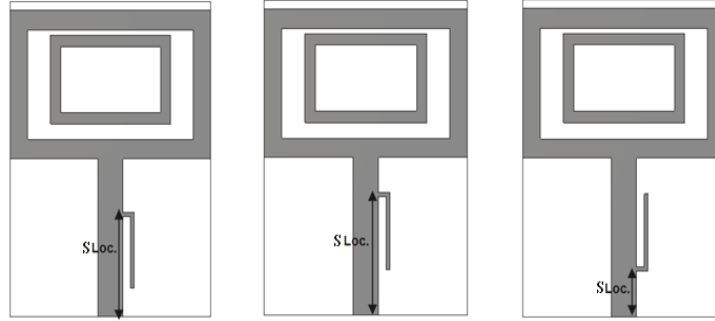


Figure 18. Geometry of dual rectangular ring antenna with $\lambda/4$ stub etched at three different locations along the feed line

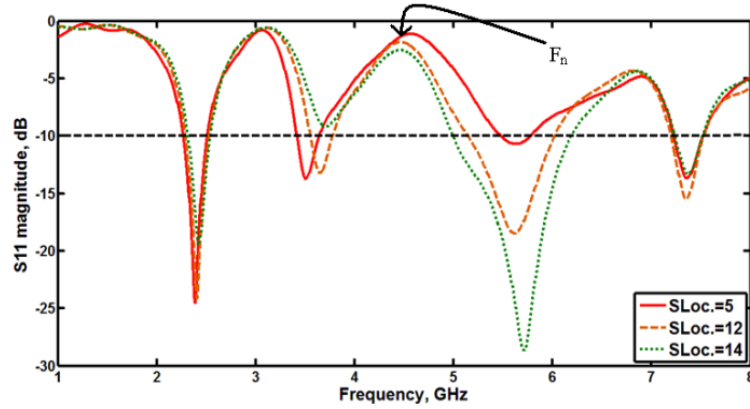


Figure 19. Reflection coefficient characteristic for several locations of the $\lambda/4$ stub along the feed line

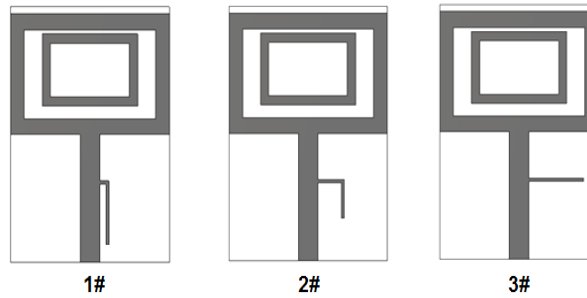


Figure 20. Geometry of dual rectangular ring with 3 shapes of the $\lambda/4$ stub

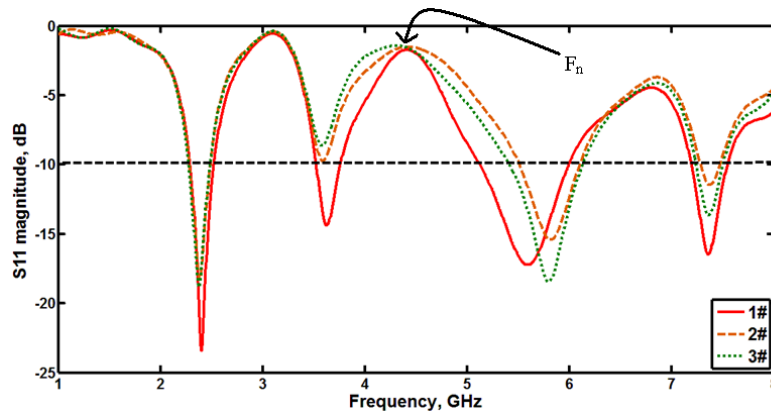


Figure 21. Reflection coefficient characteristics for the 3 shapes of the $\lambda/4$ stub

6. Comparison Between the Three Band Notch Techniques

A comparison between the performance of the three band reject techniques investigated in this paper is shown in Table (8). The use of the $\lambda/4$ stub provides the highest reflection coefficient as compared to the other two methods. The U-shape slot and the $\lambda/4$ stub have the ability to control the notch band by varying the width of the slot or the stub. The U-shape slot has no effect on the size of the antenna but the stub and the parasitic element suffer from increased complexity and possibly increased size of the antenna if they are not placed properly.

Table 8. Comparison between the performance of the three band-notch techniques

Method	F_n (GHz)	Reflection coefficient at F_n (dB)	Effect on the two bands	General comments
Parasitic element	4.5	-3.6	Increases the reflection coefficient at the first band and almost has no effect on second band	Can offer many notched-bands
U-Shaped slot in feed line	4.33	-3.1	Increases the reflection coefficient at the first band and almost has no effect on second band	Difficult to implement more than one notched band
$\lambda/4$ stub	4.46	-1.54	Shifts the first band to lower value and increases the reflection coefficient at the second band	Can offer many notched-bands

7. Conclusions

Three known band-notching techniques have been investigated by computer simulations. They include the use of; parasitic elements, slots, and stubs. For the three approaches considered, the added element is designed to resonate at the notch frequency. At the notch band, the added element disturbs the current distribution in the radiating patch leading to reduced radiation. In an alternative approach the added element produces high reflection coefficient at the notch frequency. It was shown that, the use of the $\lambda/4$ stub provides the highest reflection coefficient as compared to the other methods. The U-shape slot and the $\lambda/4$ stub have the ability to control the width of notch band by varying the width of the slot or the stub. The U-shape slot has no effect on the size of the antenna but the stub and the parasitic element increases the complexity and possibly will increase the size of the antenna if they are not properly placed.

REFERENCES

- [1] Kim, K-H, S-O Park, "Analysis of the small band-rejected antenna with the parasitic strip for UWB", IEEE Trans. Antennas Propag., Vol. 54, No.6, PP. 1688–1692, 2006.
- [2] Lin, Y.C., K.J. Hung, "Compact ultra wideband rectangular aperture antenna and band- Notched design", IEEE Trans Antennas Propagat. Vol. 54, PP. 3075–3081, 2006.
- [3] Neyestanak, A.A. L., and A.A. Kalteh, "Band-notched elliptical slot UWB microstrip antenna With elliptical stub filled by the H-shaped slot", Journal of Electromagnetic Waves & Application, Vol. 22, No.14-15, PP. 1993–2002, 2008.
- [4] Fallahi, R. A. A. Kalteh, M.G. Roozbahani, "A novel UWB elliptical slot antenna with band- notched characteristics", Progress In Electromagnetics Research PIER, Vol. 82, PP.127–136, 2008.
- [5] Lizzi, L. and A. Massa, "Dual-band printed fractal monopole antenna for LTE applications", IEEE Trans. on Antennas and Wireless Propagation Letters, Vol. 10, PP.760-763, Aug. 2011.
- [6] Barbarino, S. and F. Consoli, "UWB circular slot antenna provided with an inverted-L notch filter for the 5 GHz WLAN band", Progress In Electromagnetics Research, Vol. 104, PP.1-13, 2010.
- [7] Li, C.-M. and L.-H. Ye, "Improved dual band-notched UWB slot antenna with controllable notched band-widths," Progress In Electromagnetics Research, Vol. 115, PP. 477-493, 2011.
- [8] Qu, S., J. Li, and Q. Xue, "A band-notched ultra wideband printed monopole antenna", IEEE Trans. on Antennas and Wireless Propagation Letters, Vol. 5, PP. 495-498, 2006.
- [9] Q-X Chu, Y-Y Yang, "A compact ultra wideband antenna with 3.4/5.5 GHz dual band-notched characteristics", IEEE Trans. Antennas Propagat., Vol. 56, PP. 3637–3644, 2008.
- [10] Sim, C.-Y.-D., W.-T. Chung, and C.-H. Lee, "Planar UWB antenna with 5 GHz band rejection switching function at ground plane", Progress In Electromagnetics Research, Vol.106, PP.321-333, 2010.
- [11] Jiang, J., Y. Song, Z. Yan, X. Zhang, and W. Wu, "Band-notched UWB printed antenna with an inverted-L-slotted ground", Microwave. Opt. Technol. Lett., Vol. 51, PP.260-263, 2009.
- [12] Kelly, J. R., P. S. Hall, and P. Gardner, "Band-notched UWB antenna incorporating a microstrip open-loop resonator", IEEE Trans. on Antennas and Propag., Vol. 59, PP.3045-3048, 2011.
- [13] Thomas, K. G. and M. Sreenivasan, "A simple ultra wideband planar rectangular printed antenna with band dispensation", IEEE Trans. on Antennas and Propag., Vol. 58, PP.27-34, 2010.
- [14] Abbosh, A. M. and M. E. Bialkowski, "Design of UWB planar band-notched antennas using parasitic elements", IEEE Trans. on Antennas and Propag., Vol. 57, PP.796-799, 2009.

- [15] Zhao, Y.H., J.P. Xu, and K. Yin, "Dual band-notched ultra-wideband microstrip antenna using asymmetrical spur lines", *Electronic Letters* Vol.44, No.18, PP. 1051–1052, 2008.
- [16] Lin, C-C., P. Jin, and W. Ziolkowski, "Single, dual and tri-band-notched ultra wide band (UWB) antennas using capacitively loaded loop (CLL) resonators", *IEEE Trans. on Antennas and Propag.*, Vol. 60, PP. 102-109, 2012.
- [17] Panda, J. R. and Kshetrimay, R. S., "A 3.4/5.5 GHz Dual-Band Notched UWB Printed Monopole Antenna with Two Open-Circuited Stubs in The Microstrip Feed Line", *Microwave and Optical Technology Letters*, Vol. 53, No. 12, Dec. 2011, pp. 2973-2978.
- [18] Li, C. M., and L. H. Ye, "Improved Dual Band-Notched UWB Slot Antenna With Controllable Notched Band-Widths", *Progress In Electromagnetics Research*, Vol. 115, PP.477-493, 2011
- [19] Zhang, K., T. Wang, and L. Cheng, "Analysis of band-notched UWB printed monopole antennas using a novel segmented structure", *Progress In Electromagnetics Research C*, Vol. 34, 13-27, 2013.
- [20] Sayidmarie, K. H., and M. E. Bialkowski, "Fractal unit cells of increased phasing range and low slopes for single-layer microstrip reflectarrays", *IET Journal on Microwaves Antennas & Propagation*, Vol. 5, No. 09, 2011, PP. 1371-1379.
- [21] Li, L., Z.-L. Zhou and J.-S. Hong, "Compact UWB antenna with four band-notches for UWB applications", *Electronics Letters*, Vol. 47, No. 22, Nov. 2011, PP.1211-1212.
- [22] Xiong, L., and P. Gao, "Dual-band planar monopole antenna for bluetooth and UWB applications with wimax and WLAN band-notched", *Progress In Electromagnetics Research Letters*, Vol. 28, 183-194, 2012.
- [23] Al Malkawi, M.J., and V.K. Devabhaktuni, "Quad band-notched UWB antenna compatible with WiMAX/INSAT/lower-upper WLAN applications", *Electronics Letters*, Vol. 47, No. 19, PP. 1062-1063, 2011.
- [24] Sayidmarie, K. H., and T. A. Nagem, "Compact dual-band dual-ring printed monopole antennas for WLAN applications", *Progress In Electromagnetics Research B*, Vol. 43, PP. 313-331, 2012.
- [25] Ren, L.-S., Li, F., Zhao, J.-J., Zhao, G. and Jiao, Y.-C., "Compact Printed Ultrawideband Monopole Antenna with Dual Band-Notched Characteristics", *J. of Electromagnetics Waves and Appl.*, Vol. 24, pp. 1521–1529, 2010.
- [26] Kim, K. H., Hwang, S. H. and Park, S. O., "Band-Notched UWB Planar Monopole Antenna with Two Parasitic Patches", *Electronics Letters*, July 2005, Vol. 41, No. 14, pp.783-785.
- [27] Zaker, R., Ghobadi, C. and Nourinia, J., "Novel Modified UWB Planar Monopole Antenna with Variable Frequency Band-Notch Function", *IEEE Antennas and Wireless Propagation Letters*, Vol. 7, 2008, pp.112-114.
- [28] Hong, Z., Jiao, Y., Yang, B. and Zhang, W., "A Dual Band-Notched Antenna For Ultra-Wideband Applications", 2011 IEEE International Conference on Microwave Technology & Computational Electromagnetics (ICMTCE), Beijing, China, 22-25 May 2011, pp. 200-202.
- [29] Pozar, D.M., "Microwave Engineering", John Wiley & Sons, Third Edition, 2005.